Analysis of Fixed Bed Sorption: Flue Gas Desulfurization

Temperature and concentration profiles are obtained by solution of the coupled nonlinear differential equations which describe transient operation of an adiabatic fixed bed reactor. The unreacted-shrinking core mechanism describes the multiple, irreversible, exothermic gas-solid reactions. Numerical integration is accomplished by a predictor-corrector scheme which is programmed in Fortran IV language. The influence of kinetic parameters, heat and mass diffusivities within pellets, temperature variation of properties, gas velocity, bed and particle dimensions, inlet gas temperature and composition, and initial bed temperature on reactor performance are studied for sulfur dioxide removal from flue gases by fixed beds of copper oxide. Comparison with commercial reactors is in qualitative agreement.

SIDNEY V. BOURGEOIS, JR.
FRANK R. GROVES, JR.
and
ALBERT H. WEHE

Louisiana State University
Baton Rouge, Louisiana 70803

SCOPE

Sulfur dioxide, emitted in flue gases as a result of the burning of sulfur-containing fuels, is a major air pollutant in the United States. A number of processes for removal of sulfur dioxide from stack gas are under intense study. One of these processes, the fixed bed sorption process, removes the sulfur dioxide by absorbing it on a bed of granular porous solid particles. The absorption occurs by reaction of the sulfur dioxide with a metal oxide (for example, cuprous oxide) distributed on the porous granules that fill the reactor.

In this study we obtain a rigorous mathematical model capable of simulating the complex mass transfer, heat transfer, and chemical reaction steps that occur in the metal oxide sorption process. The model is used to determine by simulation the effects of such variables as flue gas temperature, flue gas oxygen content, bed temperature, bed length, and particle size on the performance of a particular reactor using cuprous oxide as the sorbent. The information obtained will be of value in the selection of optimum reactor operating conditions.

CONCLUSIONS AND SIGNIFICANCE

A mathematical model of the fixed bed sulfur dioxide absorption process was obtained which includes the effects of heat and mass transfer both internal and external to the absorbent pellets. The form of the model is sufficiently general that it should be useful in simulating other fluid-solid interaction processes such as adsorption, ion exchange, and catalyst regeneration by carbon burnoff.

The model was used to simulate a fixed bed sorption process based on the reaction of sulfur dioxide with cuprous oxide. Simulation studies of process variables lead to the following conclusions for the cuprous oxide process:

1. Pore diffusion and chemical reaction of sulfur dioxide with cuprous oxide are important factors in determining the rate of the process.
2. Resistance to heat transfer within the pellets is significant.
3. Behavior of the reactor is strongly influenced by temperature and particle size of the porous absorbent. High temperature and small pellet size are desirable.
4. High inlet oxygen concentration and large pore size in the absorbent pellets are desirable but not so significant as bed temperature and pellet size.

The simulations indicate that the cuprous oxide process is feasible for absorbent pellet diameters smaller than 6 mm, inlet flue gas temperature greater than 400°C, and initial bed temperature exceeding 440°C. A temperature rise in the bed of approximately 100°C and a sulfur dioxide breakthrough time of about 20 min. can be expected under these conditions.

The purpose of this study is to develop an efficient, accurate mathematical model capable of simulating a large class of fixed bed operations. Particular attention is given to rigorous description of detailed intraparticle phenomena. Previous fixed bed simulations have tended to oversimplify these intraparticle phenomena. A system exhibiting complex intraparticle heat and mass transfer—removal of sulfur dioxide from flue gases by fixed beds of copper oxide—was chosen to demonstrate the practicality of the model.

Descriptive partial differential equations for the process are obtained by applying the conservation of mass and energy. These equations are simplified by characteristic transformations of the independent variables. The resulting equations are solved numerically on a digital computer using a predictor-corrector scheme.

Correspondence concerning this paper should be addressed to S. V. Bourgeois, Lockheed Missiles & Space Company, Inc., Huntsville Research & Engineering Center, P. O. Box 1103 West Station, Huntsville, Alabama 35807.

Sulfur dioxide has been recognized for a number of years as a major air pollutant (Bienstock et al., 1958) and is termed by some as the worst industrial air pollutant (Newell, 1966). Approximately three-fourths of the sulfur dioxide emitted in the United States is produced by electrical power plants burning fossil fuels. Upon oxidation, the natural sulfur in these fuels is converted to sulfur dioxide and released to the atmosphere as a low concentration component of flue gases.

A commercial fixed bed sorption process for removing sulfur from stack gases utilizing a regenerable solid has been announced (Dautzenberg, et al., 1971), and several moving bed schemes are under investigation (Parsons, et al., 1969). These processes involve noncatalytic, heterogeneous reactions (sorption) between the stack gases and metal oxides (sorbents) distributed in the porous reactor packing material. Mathematical simulation of a fixed bed process incorporating these reaction mechanisms leads to very complex models.

These noncatalytic solid-gas reactions can occur homogeneously throughout the solid phase or at the interface between the unreacted solid and the porous product layer (Wen, 1968). The latter mechanism is known as the shrinking-core model and Wen and Wang (1970) state that it describes sulfur dioxide sorption accurately.

In order for a gas molecule to be absorbed by the solid pellet it must:

1. Diffuse through the external boundary layer or film at the surface of the pellet;
2. Diffuse into the interior of the pellet by way of pores; and
3. React chemically with the solid at the shrinking core.

The sorption rate is influenced by all three of these mechanisms. Hence we speak of external film, pore, and chemical reaction resistances to the sorption process. The heat of reaction must be conducted from the interior of the pellet to the surface and then through the external film to the flowing gas stream. Thus, there are also pore and film resistances to heat transfer.

Few reactor models employing shrinking core kinetics have been developed. Agnew and Narsimhan (1970), K. E. Olson et al. (1968), J. H. Olson (1968), and Scott (1969) have described various models for this kind of reactor. The present work extends the previous models to include intraparticle heat effects when all three resistances to mass transfer are simultaneously significant and to enable consideration of multiple solid reactants involved in a mixed reaction scheme; that is, a combination of independent, parallel, and/or consecutive reactions. The solution algorithm was developed in a general manner and should be applicable to a wide variety of fixed bed models including reactors, adsorbers, ion exchangers, dryers, etc.

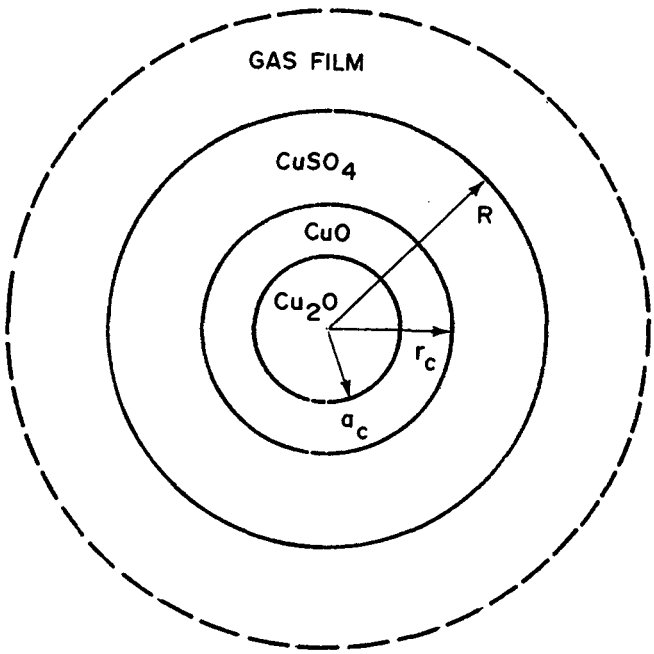

Fig. 1. Pellet phases for the Cu-S-O reactions.

MODEL DEVELOPMENT

Consider a horizontal cylindrical vessel randomly packed with uniform porous spheres. Each sphere is impregnated with a single solid reactant which is evenly dispersed throughout the pellet. The flue gas flowing in the bed consists of five components: O_2, SO_2, N_2, CO_2, and H_2O.

The stoichiometry to be used is that given by Sladek et al. (1971) and Bienstock et al. (1958) describing the irreversible exothermic reactions between cuprous oxide, oxygen, and sulfur dioxide:

$$Cu_2O + \tfrac{1}{2}\, O_2 \rightarrow 2\, CuO \qquad \text{(oxidation)}$$

$$CuO + SO_2 + \tfrac{1}{2}\, O_2 \rightarrow Cu\, SO_4 \qquad \text{(sulfation)}$$

According to Wen and Wang (1970) and Parsons et al. (1969), the foregoing solid-gas reactions can be described by the shrinking-core mechanism. A cross-sectional view of a partially reacted spherical particle would reveal three distinct layers—an outer layer of $CuSO_4$, an intermediate layer of CuO, and an unreacted inner core of pure Cu_2O. If oxidation is much faster than sulfation, the situation illustrated in Figure 1 exists. A sphere of radius R is surrounded by a gas film offering resistance to mass transfer. In the outer portion of the sphere r_c to R, both reactions have occurred and in another section a_c to r_c, only the oxidation reaction has occurred. An inner core of unreacted pellet exists from the center of a pellet to radius a_c. Both the inner solid phase interface a_c and the outer solid phase interface radius r_c are moving inward with respect to time, while the pellet outside radius R is constant.

The following assumptions can be justified for flue gas sulfur removal via sorption in fixed bed reactors (Bourgeois, 1972):

1. The fluid stream is in plug flow with negligible pressure loss between the entrance and the exit of the bed.
2. Radial convection of energy and mass are negligible.
3. Radial diffusion of mass and radial conduction of heat are negligible.
4. Axial dispersion of heat and mass are negligible.
5. Thermal equilibrium exists between the solid and gas within the pellets.
6. Radial symmetry exists within each spherical pellet.
7. Radiation and conduction between adjacent pellets is negligible.
8. Accumulation of mass within the pellet pores is negligible in comparison to the reaction rates at the shrinking core interfaces (pseudo steady state approximation).
9. The mass velocity and molecular weight of the bulk gas stream are constant.
10. No temperature or pressure gradients exist within the pellets.

The rate of oxygen consumption R_I, at the oxidation reaction site within a pellet is given by

$$R_I = k_I y_{s1} \tag{1}$$

where y_{s1} is the pellet gas phase mole fraction of oxygen. The rate of sulfur dioxide consumption R_{II} at the sulfation reaction site within a pellet is given by

$$R_{II} = k_{II} y_{s1} y_{s2} \tag{2}$$

where y_{s2} is the pellet gas phase mole fraction of sulfur dioxide. Both of the preceding reaction rate expressions have been experimentally and/or theoretically justified (Parsons et al., 1969 and Bourgeois, 1972).

Using the preceding rate expressions and the assumptions noted above, material and energy balances can be made on a section of reactor and on individual particles to give partial differential equations that describe the behavior of the reactor. Details of the derivation are available in Supplement A* and in Bourgeois (1972).

The final equations in dimensionless form are

$$\frac{\partial \psi}{\partial \lambda} = \frac{-3(1-\epsilon)Lh}{GRC_g}(\psi - \Theta) \tag{3}$$

$$\frac{\partial Y}{\partial \lambda} = \frac{-3(1-\epsilon)\rho_g K_1 L}{GR}\overline{\Delta Y} \tag{4}$$

$$\frac{\partial S}{\partial \lambda} = \frac{-3(1-\epsilon)\rho_g K_2 L}{GR}\overline{\Delta S} \tag{5}$$

$$\frac{\partial \phi}{\partial \theta} = \frac{-\epsilon \rho_g \beta k_I y_1^0 L}{GR\rho_s W_6}\overline{YAC} \tag{6}$$

$$\frac{\partial \omega}{\partial \theta} = \frac{-\epsilon \rho_g \alpha k_{II} y_1^0 y_2^0 L}{GR\rho_s W_7}\overline{YRC}\;\overline{SRC} \tag{7}$$

$$\frac{\partial \Theta}{\partial \theta} = \frac{-3\epsilon\rho_g Lh}{GR\rho_s C_s}\left[(\Theta - \psi)\frac{K_1 \Delta H_I y_1^0}{hT_0}\overline{\Delta Y} + \frac{K_2(\Delta H_{II} - \gamma \Delta H_I) y_2^0}{hT_0}\overline{\Delta S}\right] \tag{8}$$

The variables Θ, ψ, Y, and S represent the dimensionless pellet temperature, bulk gas phase temperature, oxygen concentration, and sulfur dioxide concentration, respectively. These variables are normalized by the inlet conditions of the bed. The location of the oxidation reaction interface a_c and the sulfation reaction interface r_c within the pellets are given in terms of the dimensionless radii ϕ and ω, respectively. The remaining parameters in these equations represent physical properties of the reactor system and are defined in the Notation. The barred quantities, $\overline{\Delta Y}$, $\overline{\Delta S}$, $\overline{YAC}$, $\overline{YRC}$, and $\overline{SRC}$, are defined in Appendix A.

The dimensionless position and time independent variables are characteristic variables defined by

$$\lambda = z/L$$

$$\theta = \frac{Gt}{\rho_g \epsilon L} - \frac{z}{L}$$

where z and t represent dimensioned axial bed distance and time respectively.

The normalized, dimensionless boundary and initial conditions for the preceding differential equations follow.

* Supplement A has been deposited as Document No. 02293 with the National Auxiliary Publications Service (NAPS), c/o Microfiche Publications, 305 E. 46 St., N. Y., N. Y. 10017 and may be obtained for $1.50 for microfiche or $2.00 for photocopies.

TABLE 1. PHYSICAL PROPERTIES WITH TEMPERATURE EFFECTS

Property	Expression*	Value at 675°K, 1 atm	Units
ρ_g	$0.351T^{-1}$	$5.2 \cdot 10^{-4}$	g/cc
C_g	$0.228 + 8.33 \cdot 10^{-5}T + 3.04 \cdot 10^{-9}T^2$	0.286	cal/g-°K
C_s	$0.207 + 8.14 \cdot 10^{-5}T - 3130T^{-2}$	0.256	cal/g-°K
D_{e1}	$3.69 \cdot 10^{-4}T^{0.562}$	0.0144	cm²/s
D_{e2}	$3.71 \cdot 10^{-4}T^{0.509}$	0.0102	cm²/s
h	$8.85 \cdot 10^{-5}T^{0.445}$	$1.61 \cdot 10^{-3}$	cal/cm²-s-°K
ΔH_I	$2.61T - 67500$	−65740	cal/mole O_2
ΔH_{II}	$7.41T - 138640$	−133600	cal/mole SO_2
k_I	$9.15 \cdot 10^6 e^{\left(\frac{-1350}{T}\right)}$	$1.24 \cdot 10^6$	cm/s
k_{II}	$8.92 \cdot 10^{14} e^{\left(\frac{-13500}{T}\right)}$	$1.84 \cdot 10^6$	cm⁴/mole-s
K_1	$2.16 \cdot 10^{-3}T^{1.31}$	10.99	cm/s
K_2	$8.39 \cdot 10^{-4}T^{1.41}$	8.19	cm/s

* Where T = °K.

At the bed inlet, fixed concentrations and constant inlet temperature exist,

$$\psi(0, \theta) = Y(0, \theta) = S(0, \theta) = 1.0 \tag{9}$$

and at the instant flue gas is admitted to the bed, a uniform initial bed temperature and completely unreacted pellets exist,

$$\phi(\lambda, 0) = \omega(\lambda, 0) = 1.0 \tag{10}$$

$$\Theta(\lambda, 0) = T_i/T_0 \tag{11}$$

where T_i represents the initial bed temperature and T_0 the inlet flue gas temperature. These conditions are chosen for convenience, but time varying inlet conditions and spatially dependent initial conditions could also have been specified without rendering the equations intractable.

Each of the characteristic differential equations involves differentiation with respect to only a single independent variable. Hence they can be solved by simple extensions of methods used for ordinary differential equations. In this study a predictor-corrector algorithm was used for the numerical solution (Bourgeois, 1972).

RESULTS AND DISCUSSION

In addition to concentration and temperature profiles, the maximum bed temperature and breakthrough time are important parameters. Breakthrough time will be defined as the time required for the sulfur dioxide level at the exit of the reactor to increase to 10% of its inlet concentration. Larger breakthrough times mean less frequent regeneration and more economical operation. The maximum allowable peak bed temperature is 750°C to prevent degradation of the pellets (Bourgeois, 1972).

Operating Parameters

Expressions for the physical properties of the flue gas and the porous pellets consisting of copper oxide distributed on an inert alumina carrier are presented in Table 1. Values for these properties at 400°C are also given since 400°C and 1 atm. will represent standard operating conditions. Standard values for the remaining physical properties and operating conditions are given in the Notation.

These values and expressions are the basis for the solutions to be presented unless stated otherwise. Published

data on this process are not available, but these conditions are thought to be typical (Bourgeois, 1972).

Constant Properties

Results of the numerical integration of Equations (3) to (8) by the predictor-corrector scheme are presented in Figures 2 through 7. None of the physical properties are allowed to vary with temperature. To achieve stable solutions, it was necessary to reduce $\Delta\theta$ to 10.0 for a distance step size of $\Delta\lambda = 0.05$. These step sizes were also used in the remaining cases studied unless stated otherwise. The standard initial and inlet conditions were used. For a sorption cycle of 5 min., execution time on the IBM-360-65 was 1.81 min. which corresponds to a computer/real time ratio of 0.36.

The breakthrough curve is the bottom curve in Figure 4. The normalized sulfur dioxide concentration slowly falls from its inlet concentration to a normalized value of 0.499 after 5 min. ($\theta = 782$). This can be explained by observing the exit O_2 concentration profile which is given by the bottom curve of Figure 3. It slowly increases from near 0.0. Physically, this means that the sulfation reaction cannot start immediately because most of the O_2 is being consumed by oxidation and there is very little CuO for sulfation. As more oxygen becomes available, the oxida-

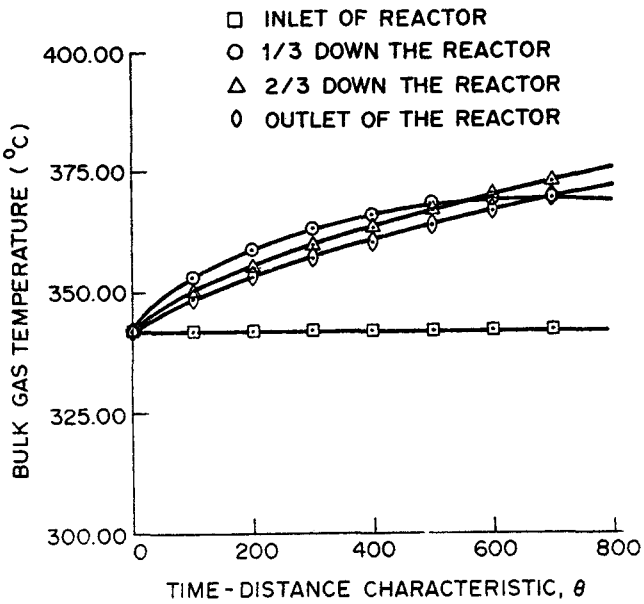

Fig. 2. Bulk gas phase temperature profiles (constant properties).

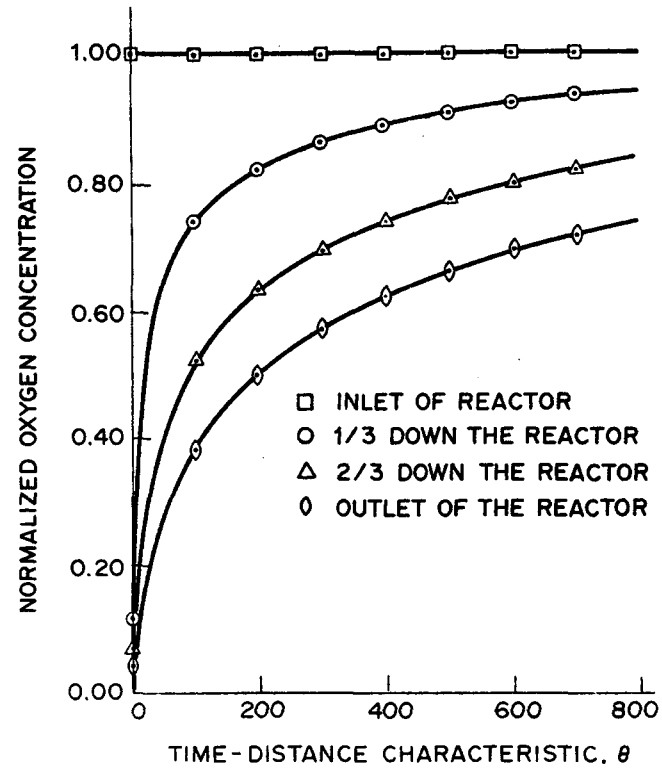

Fig. 3. Normalized oxygen profile (constant properties).

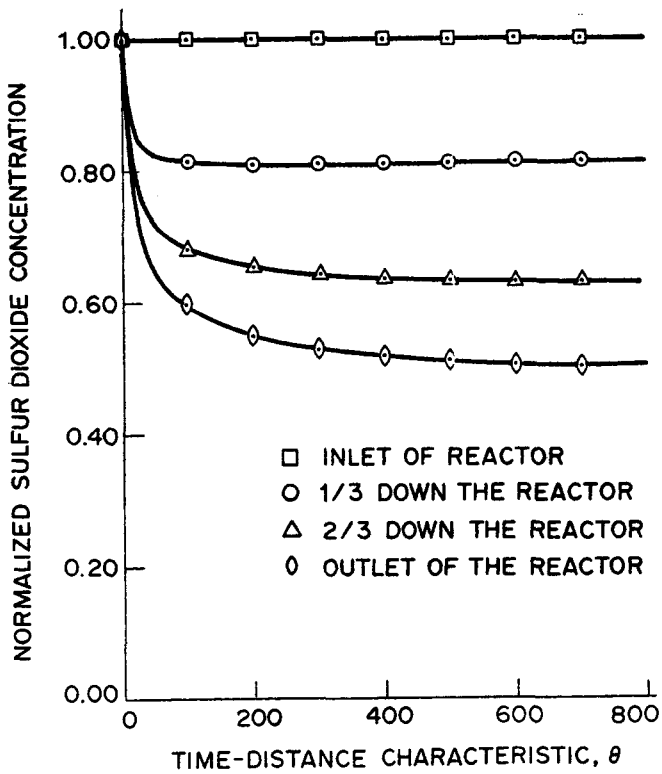

Fig. 4. Normalized sulfur dioxide profile (constant properties).

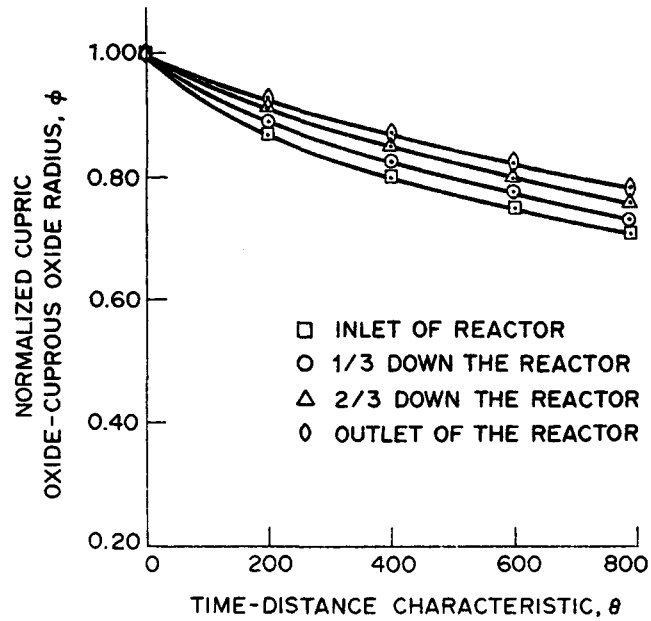

Fig. 5. Normalized oxidation reaction site penetration (constant properties).

tion reaction site penetration deepens, thereby allowing sulfation to occur. Thus, the consumption of SO_2 is delayed until the oxidation reaction penetration becomes significant. This characteristic, termed "spiking," has been observed in industrial operation of this type system (Dautzenberg et al., 1971).

Analysis of the dimensionless numbers evaluated at standard conditions will lend further insight to these results. The Sherwood numbers are both greater than 10^3 which means that resistance to diffusion of mass across the surface film surrounding each pellet is negligible compared to the resistance to mass transfer in the pellet pores. The modified Damkohler number for the oxidation reaction is on the order of 10^7 implying that the diffusion resistance in the pores is very large in comparison to resistance to the oxygen consumption at the oxidation reaction site. Thus, pore diffusion is the controlling resistance for the oxidation reaction at the standard conditions. The modified Damkohler numbers for the sulfation reaction possess orders of magnitude of 1 and 10. Thus, N_{D21}, N_{D22} and N_{Sh2} indicate that pore diffusion and chemical reaction at the sulfation site influence the sulfation reaction simultaneously and that the film mass transfer resistance is negligible. Also since $N_{D2j}/N_{D1} > 10^5$, the oxidation reaction is much faster than sulfation as was expected.

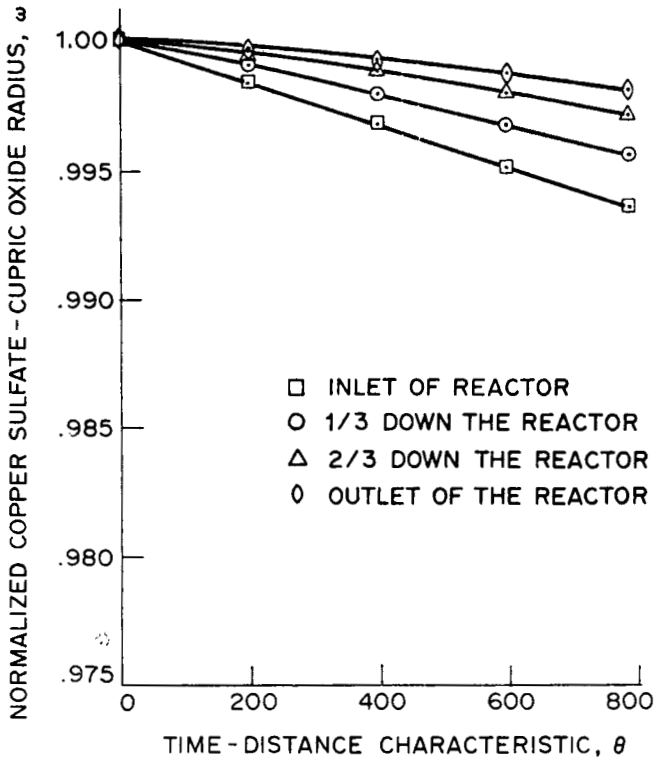

Fig. 6. Normalized sulfation reaction site penetration (constant properties).

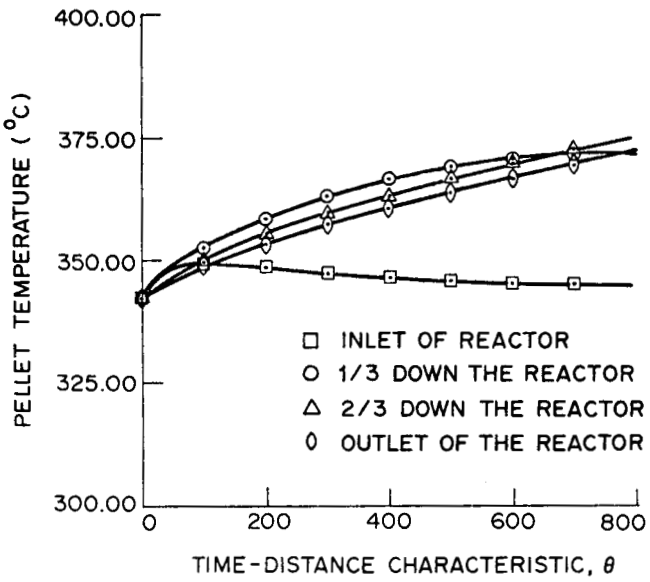

Fig. 7. Pellet temperature profiles (constant properties).

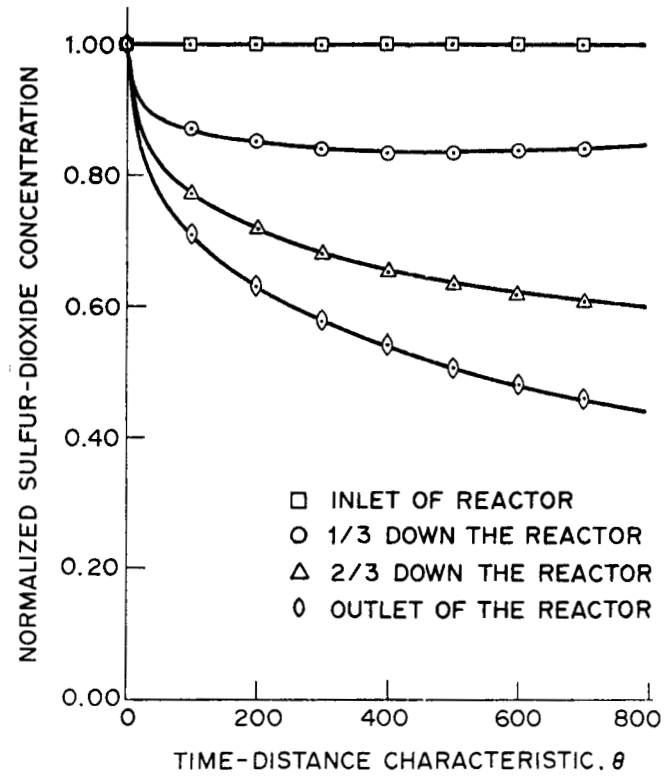

Fig. 8. Normalized sulfur dioxide profile (variable properties).

From Figure 7, the peak temperature attained by the pellets is 375°C which is a temperature rise of 33°C in 5 min. After 5 min. of sorption, the maximum sulfation reaction site penetration is $0.997R$ (1.0% pellet utilization) and the maximum oxidation reaction penetration is $0.852R$. Both conditions occur at the bed entrance as seen in Figures 5 and 6.

By increasing the sorption cycle, the exit SO_2 profile reached a minimum normalized concentration of 0.496 at 7.5 min. and then began to rise. This indicates that the point of maximum sulfation has passed through the length of the bed and finally reached the exit of the bed at 7.5 min.

Variable Properties

Figures 8 and 9 represent the variable property sulfur dioxide and pellet temperature profiles, respectively. For a 5-min. sorption cycle, the computer to real time ratio is 0.9 which is 2½ times as great as for constant properties.

The peak temperature for variable properties is 377°C which is a slight increase (2°C) in the temperature profile from the constant property case. The concentration profiles differ in that the sulfur dioxide exit profile decreases to 0.46 and is still decreasing after 5 minutes

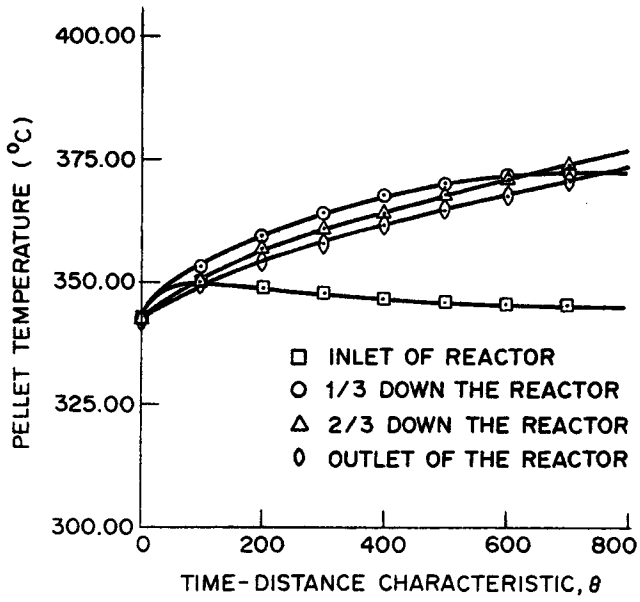

Fig. 9. Pellet temperature profiles (variable properties).

rather than leveling off to 0.50 as in the constant property run. The increased consumption of sulfur dioxide can be attributed to the slightly higher temperature level maintained throughout the course of the sorption cycle since one of the limiting resistances $1/k_{II}$ decreases strongly with temperature. The last case analyzed—general model, variable properties, 5-min. sorption cycle—will be termed Run 1.

Reaction Rate Constants

The effect of the reaction rate constants is investigated in Runs 2 through 4 as the frequency factors k_j^0 are varied. The results are tabulated in Table 2, where subscript "max" infers the maximum value attained, "min" infers the minimum value attained, the normalized sulfation reaction penetration is ω, the normalized pellet temperature is $\Theta(= T_s/T_0)$, and the normalized sulfur dioxide concentration at the exit is $S(1, \theta)$.

Each of the runs consisted of a 5-min. sorption cycle, and location for ω_{min} and Θ_{max} are at the entrance and 2/3 down the bed, respectively, and at the end of the cycle. Also in each case the minimum exit sulfur dioxide concentration occurred at the end of the cycle.

The oxidation reaction rate constant had no appreciable effect as it was varied between 10^2 and 10^{25}. In Run 4, the sulfation rate constant exhibited its rate controlling behavior as an increase of 10 times its reported value drastically changed the breakthrough curve. The shape of this curve was similar to the other runs as the exit sulfur dioxide concentration decreased from its inlet concentration, but the rate of decrease was much faster with breakthrough concentration being passed (from higher concentrations—this is not the breakthrough time) after 0.48 min. Also, as in the other runs, the exit SO_2 was still gradually decreasing after 5 min. Runs 2 and 3 indicate that assuming the value of the oxidation rate constant, k_I, is quite satisfactory.

Lumping Pellet Heat Transfer Resistance at Surface

The previous runs neglected the internal resistance to heat transfer ($k_s \to \infty$) for the pellets. The lumped (at the surface) pellet heat transfer resistance h' can be approximated by

$$\frac{1}{h'} = \frac{1}{h} + \frac{R}{k_s}$$

which yields $h'/h = 0.1$ at 400°C. Assuming that this ratio is constant with temperature, the effect of including pellet internal resistance is studied in Run 5. A comparison of the results for Runs 1 and 5 are given in Table 2.

The maximum sulfation penetration is greater in Run 5 because the inlet pellet temperatures during the entire cycle averaged 5°C higher than those in Run 1. This, coupled with the fact that the same amount of O_2 and SO_2 were available in both runs (inlet gas concentrations are

TABLE 2. PARAMETER STUDY FOR THE GENERAL MODEL WITH TEMPERATURE-DEPENDENT PHYSICAL PROPERTIES FOR FIVE-MIN. SORPTION CYCLES

Run no.	Parameter varied	Pellet utilization, ω_{min}[a]	Peak temp., Θ_{max}	Location of Θ_{max} λ	Location of Θ_{max} t(min)	Final exit SO_2 level, $S(1, \theta_f)$	Minimum exit SO_2 level, $S(1, \theta)_{min}$	Minimum exit SO_2 level, t(min)
1		0.9985	1.050	2/3	5.0	0.4380	0.4380	5.0
2	$k_I^0/k_I^{0*} = 10^{18}$[b]	0.9985	1.055	2/3	5.0	0.4380	0.4380	5.0
3	$k_I^0/k_I^{0*} = 10^{-5}$	0.9985	1.055	2/3	5.0	0.4380	0.4380	5.0
4	$k_{II}^0/k_{II}^{0*} = 10$	0.9910	1.056	2/3	5.0	0.0140	0.0140	5.0
5	$h/h^* = 10^{-1}$	0.9982	1.044	1	5.0	0.6248	0.6247	4.88
6	$T_i - T_i^* = 60$°C	0.9979	1.154	2/3	5.0	0.0790	0.0770	4.1
7	$T_i = T_0 = 755$°K, $T_i^* = T_0^* = 615$°K	0.9872	1.047	1/3	5.0	0.0003[c]	0.0002	2.5
8	$y_1^0/y_1^{0*} = 1.5$	0.9978	1.069	2/3	5.0	0.253	0.253	5.0
9	$y_2^0/y_1^{0*} = 2.0$	0.9971	1.058	2/3	5.0	0.462	0.462	5.0
10	$y_1^0/y_2^{0*} = 1.5$, $y_2^0/y_2^{0*} = 2.0$	0.9957	1.072	2/3	5.0	0.265	0.265	5.0
11	$D_{ei}/D_{ei}^* = 10$	0.9982	1.118	2/3	5.0	0.153	0.153	5.0
12	$R/R^* = 0.8$	0.9982	1.066	2/3	5.0	0.324	0.324	5.0
13	$R/R^* = 0.5$	0.9971	1.097	1/3	4.92	0.070[d]	0.070	5.0
14	$L/L^* = 2.0$	0.9985	1.056	1/3	5.0	0.260	0.260	5.0
15	$G/G^* = 0.5$	0.9985	1.055	1/3	5.0	0.256	0.256	5.0
16	$G/G^* = 1.5$	0.9985	1.056	2/3	5.0	0.256	0.256	5.0

[a] Occurs at bed inlet and end of sorption cycle in each run. Maximum pellet utilization = $1 - \omega^3_{min}$.
[b] Starred quantities represent "standard" values used in Run 1.
[c] Decreased past breakthrough level after 10 seconds.
[d] Decreased past breakthrough level after 4.1 minutes.

constant), leads to increased sulfation at the inlet. From the location and magnitude of $T_{s,max}$ in these two runs, the temperature wave for Run 5 travels down the bed faster and with a smaller amplitude than in Run 1.

Results of Run 5 indicate that rapid transfer of heat between phases aids performance of the reactor. Unfortunately, large resistance to heat transfer between the phases does exist for the present system. Thus, the profiles of Run 5 are more likely to occur than those of Run 1.

Greater Initial Bed Temperature

The effect of permitting the initial temperature of the pellets to be greater than the inlet gas temperature is studied in Run 6. The results for this 5-min. sorption cycle are shown in Table 2.

The velocity of the heat wave was not affected in Run 6 as it was in Run 5. A vastly improved breakthrough curve is obtained for Run 6. The exit SO_2 decreases rapidly from its inlet level and passes down through breakthrough after 1.8 min., reaches a minimum level at 4.1 min., then gradually begins to increase again. The peak temperature attained is 437°C which is well below the upper safety limit of 750°C.

It is very likely that industrial application of this reactor would involve initial bed temperatures greater than the inlet temperatures (Parsons et al., 1969). Therefore, this improvement in operation can be expected to occur.

Inlet Conditions

The effects of various inlet conditions are illustrated in Runs 7, 8, 9, and 10 which are compared to Run 1 in Table 2. Each of these runs represents a sorption cycle of 5 min. Inlet gas temperature and initial pellet temperature were increased from 342° to 400°C in Run 7. This corresponds to operating with a hotter flue gas. In Run 8, the inlet oxygen concentration is increased by 50%, while in Run 9 the inlet sulfur dioxide concentration is doubled over that of Run 1. For Run 10, the SO_2 and O_2 concentrations are both doubled over that of Run 1.

The velocity of the heat wave has been slowed in Run 7, since the location of $T_{s,max}$ at 5 min. is one third down the bed versus two-thirds for Runs 8, 9, 10, and 1. Run 7 possesses the best breakthrough curve of all the cases studied. The exit sulfur dioxide concentration decreased from its inlet level to the breakthrough level in ten sec. and reduced another tenfold in the next 20 sec. It then gradually declined to a minimum normalized concentration of $1.8 \cdot 10^{-4}$ after 2.5 min. At the end of the 5-min. sorption cycle it had only reached a level of $3.0 \cdot 10^{-4}$. Therefore, obtaining a hotter flue gas greatly improves breakthrough. The flue gas temperature, however, may be beyond the feasible control of the sorption unit operators; thus, this benefit may be difficult to achieve economically.

From the results of Runs 8, 9, and 10, it can be concluded that increasing the inlet oxygen concentration improves the reactor performance while increasing the sulfur dioxide concentration has no appreciable effect.

Increasing inlet O_2 concentration by 50% halved the exit sulfur dioxide concentration at the end of the 5-min. cycle. This may be a very practical method to increase the SO_2 consumption since the inlet O_2 concentration may be increased by combustion of the fuel with more excess air. This would also increase the sorber inlet temperature of the flue gas which is very desirable.

Bed, Pellet, and Pore Dimensions

Parameters which the reactor designer has some measure of control over are the bed length L, the pellet radius R and, to some extent, the pore size. Increasing the pore size is equivalent to increasing the effective diffusivities in the present system since Knudsen diffusion predominates. The effect of increasing diffusivity is given by Run 11, varying the pellet diameter is illustrated in Runs 12 and 13, and increasing bed length is studied in Run 14. These runs are compared to Run 1 in Table 2.

In Run 11, the diffusivities are made ten times greater. Such a large increase is realistic when pore size is increased to the point where ordinary molecular diffusion predominates over Knudsen diffusion. From Table 2 it can be seen that the maximum utilization of the pellets and the location of the peak temperature are equal between Runs 1 and 11. The latter fact indicates that the heat waves had equivalent velocities in each run. The peak temperature for larger pores is 39°C greater, however, which is due to the increased rate of reaction (pore diffusion was a rate limiting factor for sulfation). This caused the exit sulfur dioxide level to be much lower at the end of the cycle (0.15 versus 0.44), but still not below the breakthrough concentration. As in Run 1, the exit sulfur dioxide concentration continued to gradually decrease at the end of 5 min. in Run 11. Thus, while increasing the pore size improved the performance significantly, this factor alone will not produce practical breakthrough curves.

Reducing the pellet diameter from 12.7 to 6.4 mm is studied in Run 13 and to 10.2 mm is presented in Run 12. Reducing particle size vastly improved performance of the reactor. This is predicted by analysis of the dimensionless numbers since rates of change of each of the system dependent variables varies inversely with R. These last two numbers are the ratio of the pore diffusional resistance to film and reaction rate resistances, respectively, and a decrease in their value increases pore diffusion rates. Since pore diffusion is limiting, reducing R directly improves reaction rate according to the form of the differential equations.

In Run 12 a 20% reduction in pellet diameter resulted in a 30% drop in exit sulfur dioxide concentration when compared to Run 1 at the end of 5 min. The maximum pellet utilization and velocity of the heat wave are the same as Run 1, but the peak temperature is 7°C higher in Run 12. In Run 13 a 50% reduction in pellet diameter resulted in an 85% drop in final exit sulfur dioxide concentration. As in Run 1, the exit sulfur dioxide was gradually decreasing at the end of the cycle. Maximum pellet utilization was slightly improved in Run 13. Also in relation to Run 1, the peak temperature is 25°C greater in Run 13, and from the respective location of their peak temperatures, the velocity of the heat wave is slower in Run 13.

In Run 14, doubling the reactor length reduced the final exit sulfur dioxide concentration of Run 1 by 44% at the end of equivalent sorption cycles. The magnitude and velocity of the heat waves and the maximum pellet utilization of Runs 1 and 14 are equivalent. The comparison between Runs 1 and 14 indicates that increasing reactor length improves reactor performance, but capital investment increases with reactor size also.

In conclusion, the results of Runs 11, 12, 13, and 14 demonstrate that increasing reactor length and pore size improve the reactor performance, but not to the degree that reducing pellet diameter achieves.

The length of the sorption cycle was increased for Run 13 and resulted in a breakthrough time of 18.2 min. The pellet temperature profile and sulfur dioxide profiles for this run are presented in Figures 10 and 11, respectively.

The peak temperature is 442°C which represents a temperature rise of 100°C in 17 min. The breakthrough curve in Figure 11 remains below the 10% level for 14 min. out of the 18-min. sorption cycle.

Mass Velocity

The effect of reducing the mass velocity G is studied in Run 15, while increasing the velocity is incorporated in Run 16. The results of these studies are tabulated in Table 2 and compared to Run 1 for a 5-min. sorption cycle.

Increasing the mass velocity corresponds to either increasing the mass flow rate of the gas or reducing the cross-sectional area of the bed. In Run 16, increasing the standard value of G from Run 1 by 50% reduced reactor performance, since the exit SO_2 level increased by 32% over that of Run 1 at the end of a 5-min. sorption cycle. Halving the standard value of G increased reactor performance by reducing the exit SO_2 level of Run 1 by 44%. The magnitude of the maximum pellet utilization ($1 - \omega^3_{min}$) was not appreciably changed by varying G.

The mass flow rate of the flue gas will normally be beyond the control of the reactor designer, therefore varying G can only be accomplished by varying the bed diameter. Decreasing G by one-half corresponds to increasing bed diameter by 41% for a given gas mass rate. Therefore, this increase in performance can be achieved by increasing capital investment (larger reactor), but the increase in performance is not as significant as that produced by using smaller pellets or by increasing the bed temperature level.

CONCLUSIONS

Analyzing the system under study through use of the dimensionless constants and many simulations, it was found that:

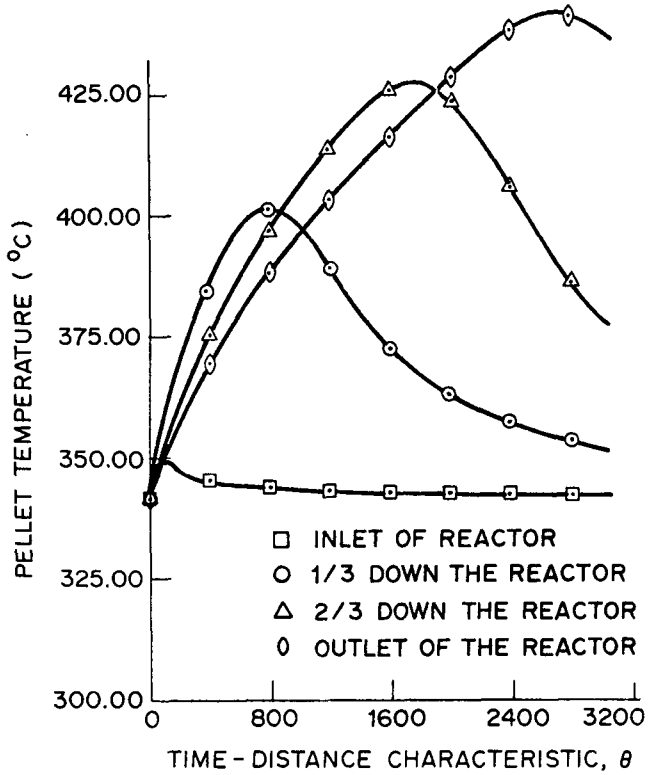

Fig. 10. Pellet temperature profiles for Run 13 (6.4 mm pellets).

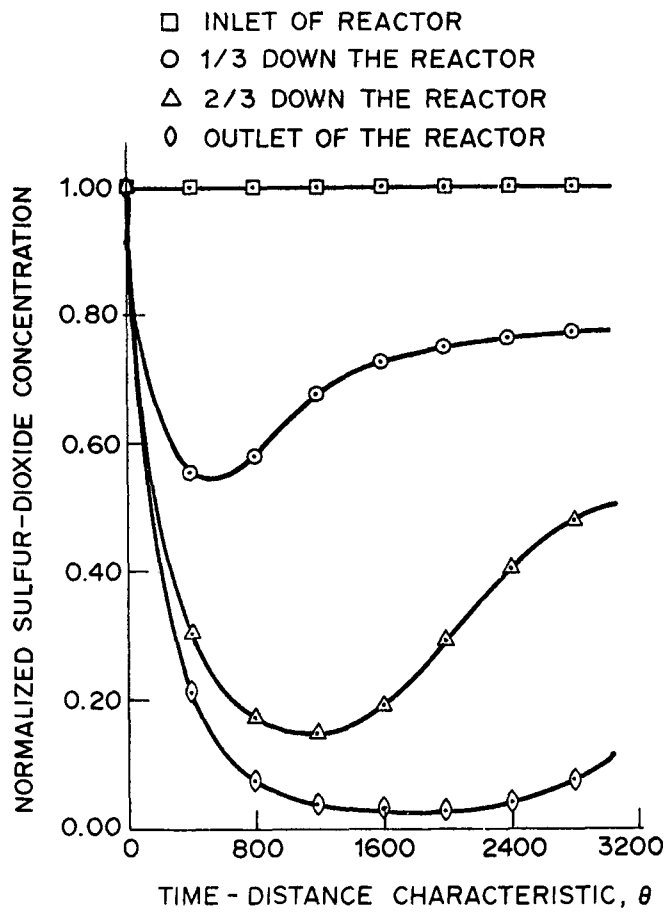

Fig. 11. Normalized sulfur dioxide profile for Run 13 (6.4 mm pellets).

1. Pore diffusion and chemical reaction in the sulfation layer of the pellets are the rate controlling factors.
2. Resistance to heat transfer within the pellets is significant, and including this resistance significantly worsens reactor performance.
3. Consumption of sulfur dioxide by the bed is very sensitive to temperature and pellet radius. Therefore, utilizing a bed still hot from regeneration, obtaining flue gas as hot as possible, and using 6.4 mm pellets or smaller are very desirable.
4. Accurate experimental determination of the sulfation activation energy and frequency factor are essential. Similarly, accurate estimation of the effective diffusivities for O_2 and SO_2, either experimentally or theoretically, is required.
5. Increasing pore size (so that molecular rather than Knudsen diffusion predominates), inlet oxygen concentration, and reactor size also improve reactor performance, but are not as significant or practical (ease of implementation and cost) as utilizing smaller pellet sizes and higher initial bed temperature and inlet flue gas temperature.

This analysis emphasized the optimization of design aspects for the system under study but could also serve in the analysis of experimental data from a pilot plant reactor. From the various simulations performed, it can be concluded that removal of SO_2 from flue gas is feasible in fixed bed reactors if pellet diameters smaller than 6.4 mm, inlet flue gas temperatures greater than 400°C, and initial bed temperatures exceeding 440°C are utilized in conjunction with the remaining standard conditions. Temperature rises of approximately 100°C and breakthrough times of about 20 min. can be expected.

ACKNOWLEDGMENT

Support for this work was provided by traineeships of the National Defense Education Act, National Science Foundation, and the National Aeronautics and Space Administration.

NOTATION

a_c = radial position within pellet at which oxidation reaction is occurring, cm
C_g = gas mixture heat capacity, cal/g-°C
C_s = pellet heat capacity, cal/g-°C
D_{ei} = effective pore diffusivity, cm²/s
G = mass flux or mass velocity, g/cm²-s
h = heat transfer coefficient at pellet surface, cal/cm²-s-°C
h' = lumped (internal and surface) pellet heat transfer coefficient, cal/cm²-s-°C
ΔH_i = heat of reaction for reaction i, cal/g mole
k_j = jth reaction's rate constant:
Reaction I = cm/s
Reaction II = cm⁴/g mole-s
k_s = effective pellet thermal conductivity, cal/cm-s-°C
k_j^0 = frequency factor for reaction j (same units as k_i)
K_i = film mass transfer coefficient of component i, cm/s
L = bed length, cm
N_{D1} = modified Damkohler number for oxidation reaction = Rk_I/D_{e1}
N_{D21} = modified Damkohler number for O_2 in the sulfation reaction = $Rk_{II}y_1^0/D_{e2}$
N_{D22} = Modified Damkohler number for SO_2 in the sulfation reaction = $R\gamma K_{II}y_1^0/D_{e1}$
N_{Shj} = Sherwood number = RK_j/D_{ej}
r_c = radial position within pellet at which sulfation reaction is occurring, cm
R = pellet outer radius, cm
R_i = surface reaction rate for ith reaction
S = normalized SO_2 concentration = y_2/y_2^0
t = time, s
T = temperature, °K
W_i = weight fraction of component i in the solid pellet
y_i = bulk gas phase molar concentration for component i, g mole/cc
y_i^0 = inlet bulk gas phase molar concentration
y_{si} = pellet gas phase molar concentration for component i, g mole/cc
Y = normalized oxygen concentration = y_1/y_1^0
z = axial distance from bed entrance, cm

Greek Letters

α = stoichiometric constant = $gCuSO_4$/g mole SO_2
β = stoichiometric constant = gCu_2O/g mole O_2
γ = stoichiometric constant = moles O_2/mole SO_2 for sulfation reaction
ϵ = bed void fraction
θ = a normalized characteristic direction = $Gt/\rho_g\epsilon L - z/L$
λ = normalized distance = z/L
Θ = normalized pellet temperature = T_s/T_0
ρ_g = gas density, g/cc
ρ_s = pellet density, g/cc
ϕ = normalized oxidation reaction radius = a_c/R
ψ = normalized bulk gas phase temperature = T_g/T_0
ω = normalized sulfation reaction radius = r_c/R

Subscripts and Superscript

i = designates ith component; ith reaction, or initial conditions
j = designates jth component or jth reaction
s = pellet gas phase
S = solid pellet phase
0 = inlet condition
1 = O_2
2 = SO_2
6 = Cu_2O
7 = $CuSO_4$
8 = CuO
I = oxidation reaction
II = sulfation reaction
0 = inlet condition for bulk gas phase concentrations

LITERATURE CITED

Agnew, J. B., and G. Narsimhan, "Stability of a Non-Catalytic Reaction in a Packed Bed," *Chem. Eng. Sci.*, **25**, 685 (1970).
Bienstock, D., L. W. Brumm, W. P. Haynes and H. E. Benson, "Sulfur Dioxides—Its Chemistry and Removal from Industrial Waste Gases," *Bur. Mines Inform. Circ. No. 7836* (1958).
Bourgeois, S. V., "Transient Analysis of Multiple Solid-Fluid Reactions in an Adiabatic Fixed-Bed Reactor: Removal of Sulfur Dioxide from Flue Gases," Ph.D. thesis, Louisiana State Univ., Baton Rouge (1972).
Dautzenberg, F. M., J. E. Nader and A. J. J. van Ginneken, "Shell's Flue Gas Desulfurization Process," *Chem. Eng. Progr.*, **67**, 86 (1971).
Newell, J. E., "Making Sulphur from Flue Gas," *Chem. Eng. Progr.*, **62**, 67 (1966).
Olson, J. H., "Rates of Poisoning in Fixed-Bed Reactors," *Ind. Eng. Chem. Fundamentals*, **7**, 185 (1968).
Olson, K. E., D. Luss, and N. R. Amundson, "Regeneration of Adiabatic Fixed Beds," *Ind. Eng. Chem. Process Design Develop.*, **7**, 185 (1968).
Parsons, T., G. D. Schroeder, and D. Deberry, "Applicability of Metal Oxides to the Development of New Processes for Removing SO_2 from Flue Gases," TRACOR Document No. 69-579-U, TRACOR, Austin, Texas (July 31, 1969).
Scott, C. D., "Oxidation of Hydrogen in a Helium Stream by Copper Oxide: Analysis of Combined Film and Pore Diffusion with Rapid Irreversible Reaction in a Fixed-Bed Process," *AIChE J.*, **15**, 116 (1969).
Sladek, K. J., P. S. Lowell, K. Schwitzgebel and T. B. Parsons, "Selection of Metal Oxides for Removing SO_2 from Flue Gas," *Ind. Eng. Chem. Process Design Develop.*, **10**, 384 (1971).
Wen, C. Y., "Noncatalytic Heterogeneous Solid Fluid Reaction Models," *Ind. Eng. Chem.*, **60**, 34 (1968).
———., and S. C. Wang, "Thermal and Diffusional Effects in Non-Catalytic Solid Gas Reactions," *Ind. Eng. Chem.*, **62**, 30 (1970).

APPENDIX A

The barred quantities appearing in Equations (3) through (8) are dimensionless and represent the interphase (pellet-bulk gas) driving force for SO_2 transfer $\overline{\Delta S}$, the interphase driving force for O_2 transfer $\overline{\Delta Y}$, the normalized pellet oxygen concentration at the oxidation reaction site $\overline{YAC}$, and the pellet oxygen concentration at the sulfation reaction site $\overline{YRC}$. These variables are defined as

$$\overline{YRC} = \frac{-B \pm \sqrt{B^2 - 4AC}}{2A}$$

$$A = \left[\phi - \phi^2\left(1 - \frac{1}{N_{Sh1}}\right) + \frac{1}{N_{D1}}\right]\left[\omega + \omega^2\left(\frac{1}{N_{Sh2}} - 1\right)\right]$$

$$B = \left[\phi - \phi^2\left(1 - \frac{1}{N_{Sh1}}\right) + \frac{1}{N_{D1}}\right] \Big/ N_{D21}$$

(Equation continued on next page)

$$\overline{YAC} = \frac{Y}{N_{D1}\left[\left\{\phi - \phi^2\left(1 - \frac{1}{N_{Sh1}}\right) + \frac{1}{N_{D1}}\right\} + N_{D22}\,\overline{SRC}\left\{\omega + \omega^2\left(\frac{1}{N_{Sh1}} - 1\right)\right\} \cdot \left\{\phi\left(1 - \frac{\phi}{\omega}\right) + \frac{1}{N_{D1}}\right\}\right]}$$

$$Y \cdot \frac{\left[\phi - \phi^2\left(1 - \frac{1}{N_{Sh1}}\right) + \frac{1}{N_{D1}}\right] + N_{D22}\,\overline{SRC}\left[\omega + \omega^2\left(\frac{1}{N_{Sh1}} - 1\right)\right]\left[\phi\left(1 - \frac{\phi}{\omega}\right) + \frac{1}{N_{D1}}\right] - \left[\left(\phi - \phi^2 + \frac{1}{N_{D1}}\right) + N_{D22}\,\overline{SRC}\left\{\phi\left(1 - \frac{\phi}{\omega}\right) + \frac{1}{N_{D1}}\right\}(\omega - \omega^2)\right]\frac{\Theta}{\Psi}}{\left[\phi - \phi^2\left(1 - \frac{1}{N_{Sh1}}\right) + \frac{1}{N_{D1}}\right] + N_{D22}\,\overline{SRC}\left[\omega + \omega^2\left(\frac{1}{N_{Sh1}} - 1\right)\right]\left[\phi\left(1 - \frac{\phi}{\omega}\right) + \frac{1}{N_{D1}}\right]} = \overline{\Delta Y}$$

$$+ \left[\phi\left(1 - \frac{\phi}{\omega}\right) + \frac{1}{N_{D1}}\right]$$

$$\left[\frac{N_{D22}}{N_{D21}}\left\{\omega - \omega^2\left(\frac{1}{N_{Sh1}} - 1\right)\right\} - Y\left(\omega + \omega^2\left\{\frac{1}{N_{Sh2}} - 1\right\}\right)\right]$$

$$C = \frac{-Y}{N_{D21}}\left[\phi\left(1 - \frac{\phi}{\omega}\right) + \frac{1}{N_{D1}}\right]$$

In defining these quantities, a new variable $\overline{SRC}$ appears which is the normalized pellet SO_2 concentration at the sulfation interface within the pellet. It is defined as

$$\overline{SRC} = \frac{S}{1 + N_{D21}\,(\overline{YRC})\,[\omega + \omega^2\,(1/N_{Sh2} - 1)]}$$

The expressions for the preceding variables are derived by solving the Laplace equations which result from the pseudo steady state pellet gas phase material balances and their boundary conditions (Bourgeois, 1972).

Manuscript received February 21, 1973; revision received August 17 and accepted September 4, 1973.

Salt Effects on Vapor-Liquid Equilibrium: Some Anomalies

Experimental data are presented for five systems, each consisting of water, an alcohol (methanol or ethanol), and an inorganic salt dissolved to saturation in the boiling liquid phase. The data confirm and extend knowledge of recently discovered anomalies to the general theory of salt effect in vapor-liquid equilibrium. A partial accounting for the observed anomalies is attempted based on recent advances in the understanding of the structural nature of alcohol-water mixtures.

DAVID MERANDA
and
WILLIAM F. FURTER

Department of Chemical Engineering
Royal Military College of Canada
Kingston, Ontario, Canada

SCOPE

Extractive distillation employing a dissolved salt in place of the conventional liquid solvent as the separating agent is capable of yielding higher separation efficiency, and with lower energy requirements, than conventional extractive distillation processing. A recent review of the theoretical and technical aspects of extractive distillation by salt effect has been published (Furter, 1972). Before large-scale commercialization is feasible, however, the theory of salt effect on vapor-liquid equilibrium must be better understood than at present.

When a salt is dissolved in a boiling solution of two liquid components, there are several salt effects that may occur. These include alterations in the boiling point, in the mutual solubilities of the two liquid components in each other, and in the composition of the equilibrium vapor phase. It is with the latter effect that this paper is concerned. Studies of salt effect in vapor-liquid equilibrium involve, in the simplest case, a two-component vapor phase in equilibrium with a three-component liquid phase, one of the components of the latter being the dissolved salt. The salt does not appear in the vapor.

At least until recently, it has been generally held that the presence of a salt in the liquid would result in an increase in concentration, in the equilibrium vapor, of the component in which the salt was less soluble, with

Correspondence concerning this paper should be addressed to W. F. Furter. D. Meranda is with Central Nuclear Services, Ontario Hydro-Electric Power Commission, Toronto, Ontario, Canada.